International Standard

ISO 25178-603

Geometrical product specifications (GPS) — Surface texture: Areal —

Part 603: Design and characteristics of non-contact (phase shifting interferometry) instruments

Spécification géométrique des produits (GPS) — État de surface: Surfacique —

Partie 603: Conception et caractéristiques des instruments sans contact (à interférométrie à glissement de franges)

Second edition
2025-02

Reference number
ISO 25178-603:2025(en)

ISO copyright office
CP 401 • Ch. de Blandonnet 8
CH-1214 Vernier, Geneva
Phone: +41 22 749 01 11
Email: copyright@iso.org
Website: www.iso.org

Published in Switzerland

Contents

Page

Foreword

ISO (the International Organization for Standardization) is a worldwide federation of national standards bodies (ISO member bodies). The work of preparing International Standards is normally carried out through ISO technical committees. Each member body interested in a subject for which a technical committee has been established has the right to be represented on that committee. International organizations, governmental and non-governmental, in liaison with ISO, also take part in the work. ISO collaborates closely with the International Electrotechnical Commission (IEC) on all matters of electrotechnical standardization.

The procedures used to develop this document and those intended for its further maintenance are described in the ISO/IEC Directives, Part 1. In particular, the different approval criteria needed for the different types of ISO document should be noted. This document was drafted in accordance with the editorial rules of the ISO/IEC Directives, Part 2 (see www.iso.org/directives).

ISO draws attention to the possibility that the implementation of this document may involve the use of (a) patent(s). ISO takes no position concerning the evidence, validity or applicability of any claimed patent rights in respect thereof. As of the date of publication of this document, ISO had not received notice of (a) patent(s) which may be required to implement this document. However, implementers are cautioned that this may not represent the latest information, which may be obtained from the patent database available at www.iso.org/patents. ISO shall not be held responsible for identifying any or all such patent rights.

Any trade name used in this document is information given for the convenience of users and does not constitute an endorsement.

For an explanation of the voluntary nature of standards, the meaning of ISO specific terms and expressions related to conformity assessment, as well as information about ISO's adherence to the World Trade Organization (WTO) principles in the Technical Barriers to Trade (TBT), see www.iso.org/iso/foreword.html.

This document was prepared by Technical Committee ISO/TC 213, *Dimensional and geometrical product specifications and verification*, in collaboration with the European Committee for Standardization (CEN) Technical Committee CEN/TC 290, *Dimensional and geometrical product specification and verification,* in accordance with the Agreement on technical cooperation between ISO and CEN (Vienna Agreement).

This second edition cancels and replaces the first edition (ISO 25178-603:2013), which has been technically revised.

The main changes are as follows:

— removal of the terms and definitions now specified in ISO 25178-600;

— revision of all terms and definitions for clarity and consistency with other ISO standards documents;

— addition of Clause 4 for instrument requirements, which summarizes normative features and characteristics;

— addition of Clause 5 on metrological characteristics;

— addition of Clause 6 on design features, which clarifies the types of instruments relevant to this document;

— addition of an information flow concept diagram in Clause 4;

— revision of Annex A describing the principles of instruments addressed by this document;

— addition of Annex B on metrological characteristics and influence quantities, replacement of the normative table of influence quantities with an informative description of common error sources and how these relate to the metrological characteristics in ISO 25178-600.

A list of all parts in the ISO 25178 series can be found on the ISO website.

Any feedback or questions on this document should be directed to the user’s national standards body. A complete listing of these bodies can be found at www.iso.org/members.html.

Introduction

This document is a geometrical product specification (GPS) standard and is to be regarded as a general GPS standard (see ISO 14638). It influences chain link F of the chains of standards on profile and areal surface texture.

The ISO GPS matrix model given in ISO 14638 gives an overview of the ISO GPS system of which this document is a part. The fundamental rules of ISO GPS given in ISO 8015 apply to this document and the default decision rules given in ISO 14253-1 apply to the specifications made in accordance with this document, unless otherwise indicated.

For more detailed information on the relation of this document to other standards and the GPS matrix model, see Annex C.

This document includes terms and definitions relevant to the phase shifting interferometry (PSI) instruments for the measurement of areal surface topography. Annex A briefly summarizes PSI instruments and methods to clarify the definitions and to provide a foundation for Annex B, which describes common sources of uncertainty and their relation to the metrological characteristics of PSI.

NOTE Portions of this document, particularly the informative sections, describe patented systems and methods. This information is provided only to assist users in understanding the operating principles of PSI instruments. This document is not intended to establish priority for any intellectual property, nor does it imply a license to proprietary technologies described herein.

Geometrical product specifications (GPS) — Surface texture: Areal —

Part 603:
Design and characteristics of non-contact (phase shifting interferometry) instruments

1 Scope

This document specifies the design and metrological characteristics of phase shifting interferometry (PSI) instruments for the areal measurement of surface topography. Because surface profiles can be extracted from areal surface topography data, the methods described in this document are also applicable to profiling measurements.

2 Normative references

The following documents are referred to in the text in such a way that some or all of their content constitutes requirements of this document. For dated references, only the edition cited applies. For undated references, the latest edition of the referenced document (including any amendments) applies.

ISO 25178-600:2019, *Geometrical product specifications (GPS) — Surface texture: Areal — Part 600: Metrological characteristics for areal topography measuring methods*

3 Terms and definitions

For the purposes of this document, the terms and definitions given in ISO 25178-600 and the following apply.

ISO and IEC maintain terminology databases for use in standardization at the following addresses:

— ISO Online browsing platform: available at https://www.iso.org/obp

— IEC Electropedia: available at https://www.electropedia.org/

3.1
phase shifting interferometry
PSI
method for measuring areal surface topography from the surface height dependence of an interferometric signal, whereby the interference phase is estimated from two or more digitized interference images acquired over a sequence of controlled phase shifts

Note 1 to entry: In this document, PSI refers specifically to methods that employ time-dependent *phase shifting mechanisms* (3.8). Other methods of acquiring and analysing interference patterns, including parallel or instantaneous methods using polarization or carrier fringes, are outside the scope of this document.

Note 2 to entry: ISO/TR 14999-2:2019, 6.4.4, provides further information on synchronous detection and PSI.

Note 3 to entry: PSI instruments are most often employed for measurements of optically smooth surfaces, as defined in ISO 25178-600:2019, 3.4.4.

3.2
interference objective
microscope objective adapted with a reference path and reference surface for the generation of interference patterns superimposed on the image of a sample surface

Note 1 to entry: Interference objectives are used in *PSI* (3.1) instruments that are configured as microscopes. Other configurations of PSI instruments, particularly for fields of view larger than about 10 mm, can have interferometer designs that are not based on microscope objectives.

Note 2 to entry: Annex A provides example types of interference objective in common usage.

3.3
linear phase shifting interferometry
linear PSI
PSI (3.1) method that relies on sampling an interference signal over a sequence of evenly spaced interference phase shifts

3.4
sinusoidal phase shifting interferometry
sinusoidal PSI
PSI (3.1) method that relies on sampling an interference signal over a sequence of sinusoidally-varying interference phase shifts

3.5
phase shifting interferometry algorithm
PSI algorithm
algorithm for the data processing procedure, including the mathematical equations, used to calculate the topography from two or more digitized interference images acquired over a sequence of controlled phase shifts

3.6
equivalent wavelength
λ_{eq}
constant value equal to twice the change in surface topography height that produces one full cycle of interference phase change (equivalent to one interference fringe)

Note 1 to entry: The equivalent wavelength is a definition in the context of *PSI* (3.1) for the measurement optical wavelength, defined as the "effective value of the wavelength of the light used to measure a surface" in ISO 25178-600:2019, 3.3.3.

Note 2 to entry: This definition corresponds to the measurement configuration described in Annex A. There can be different definitions for other measurement configurations.

Note 3 to entry: The equivalent wavelength can be calculated from contributions such as the light source wavelength together with other factors related to the instrument design, or can be calibrated using a procedure corresponding to the definition of the equivalent wavelength.

3.7
phase change on reflection
PCOR
change in interference phase attributable to the optical properties of a sample surface independent of surface height

Note 1 to entry: The PCOR is most relevant to non-dielectric materials such as metals and surfaces that have thin layers of differing materials producing thin-film effects.

Note 2 to entry: The PCOR can vary over the sample surface comprised of an optically non-uniform material (see ISO 25178-600:2019, 3.4.6).

3.8
phase shifting mechanism
device that imparts controlled phase shifts to an interference signal

Note 1 to entry: The phase shift mechanism can generate phase shifts by an axial scan motion of the part or of the interference objective (see ISO 25178-607:2019, 3.5), or other methods, such as displacement of the reference surface.

3.9
phase unwrapping algorithm
algorithm used to extend the surface topography measurement range beyond a single cycle of interference phase (equivalent to one interference fringe), by removing excess multiples of 2π between the phase values of neighbouring image points

Note 1 to entry: ISO/TR 14999-2:2019, 6.6, provides further details regarding phase unwrapping.

3.10
fringe-order error
2π error
<phase shifting interferometry> error in the identification of the correct fringe when calculating relative heights using interference phase for surface topography calculations

Note 1 to entry: Fringe-order errors are integer multiples of one-half the *equivalent wavelength* (3.6) in height.

4 Instrument requirements

An instrument according to this document shall perform areal surface topography measurements of a sample surface using PSI. The instrument can comprise an interference objective or alternative interferometer assembly and a phase shifting mechanism. The instrument shall acquire data using linear PSI, sinusoidal PSI or other phase shifting patterns consistent with the definition of PSI. The instrument shall convert acquired data to an areal topography using a PSI algorithm and a calculated or assumed equivalent wavelength. A phase unwrapping algorithm shall be employed as needed to reduce fringe-order error.

Figure 1 shows the information flow between these elements for a PSI microscope, from the real surface to a scale-limited surface. Example PSI hardware, techniques and error sources are given in Annexes A and B.

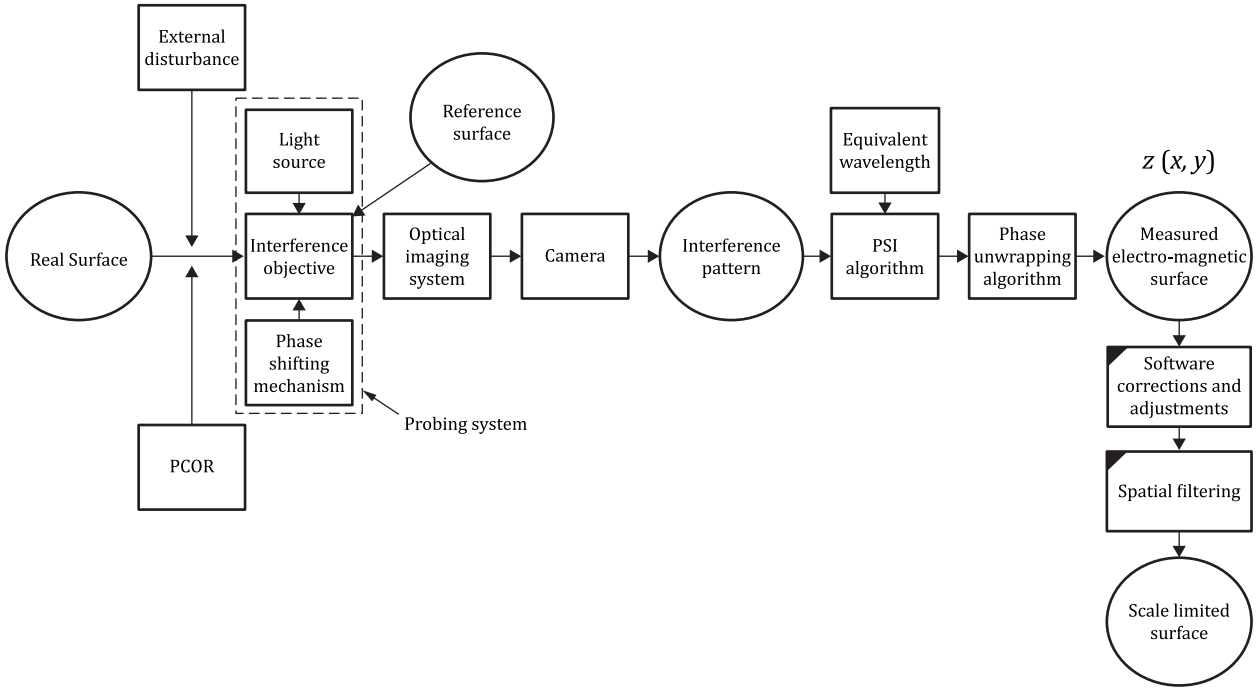

Key

measurand

operator with intended modification

operator without intended modification

Figure 1 — Information flow concept diagram for PSI

5 Metrological characteristics

The standard metrological characteristics for areal surface texture measuring instruments specified in ISO 25178-600 shall be considered when designing and calibrating the instrument.

Annex B describes sources of measurement error that can influence the calibration result.

6 Design features

Standard design features described in ISO 25178-600 shall be considered in the design.

Annex A provides examples of specific design features of PSI instruments.

7 General information

The relationship between this document and the GPS matrix model is given in Annex C.

Annex A
(informative)

Principles of PSI instruments for areal surface topography measurement

A.1 General

PSI is a mature technology and there are substantial resources in existing ISO documents listed in the bibliography and in the published literature regarding instrument design and theory of operation.[9][10][11][12][13] This annex provides a summary with the goal of clarifying terms and definitions as well as some of the influence quantities that contribute to the metrological characteristics of PSI.

A.2 Instrument design

PSI instruments for areal surface topography measurement comprise a variety of designs. The testing of optical components such as lenses, mirrors and prisms often relies on the laser Fizeau geometry, used for polished surfaces from a few millimetres to over a metre in size.[14][15] This annex describes the use of PSI together with light microscopy for areal surface topography using a mechanical phase shifting mechanism. Refer to ISO/TR 14999-1 for general terms and definitions related to light interferometry and to ISO 10934 for general terms and definitions related to light microscopy.

Figure A.1 shows an interference microscope with imaging optics. The phase shifting mechanism imparts a controlled phase shift by means of an axial scan ζ of the interference objective towards the sample surface along the *z*-axis direction (see ISO 25178-607:2019, 3.5). The sample surface lies nominally within the plane, consistent with the coordinate system defined in ISO 25178-600:2019, 3.1.2, and is imaged to the electronic camera. The measurement principle is to determine the surface height at each point on the sample surface by analysis of multiple interference patterns acquired during a sequence of controlled phase shifts.

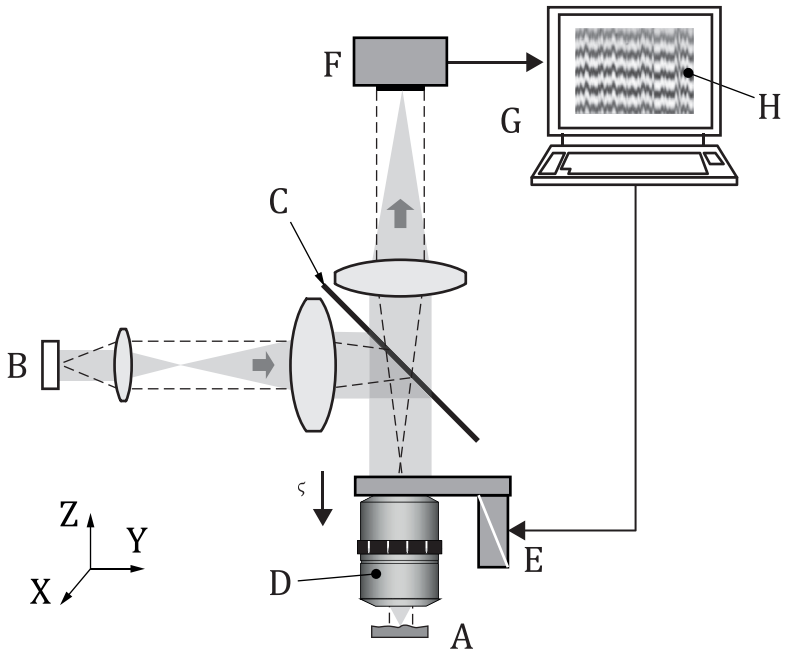

Key

A	workpiece	E	phase shifting mechanism
B	light source	F	electronic camera
C	beam splitter	G	data acquisition and control
D	interference objective	H	interference pattern
ζ	scanning motion		

Figure A.1 — Interference microscope for PSI measurements of the areal surface topography

Light sources for interference microscopy are usually spatially incoherent, exemplified by incandescent lamps or white-light-emitting diodes (see ISO 10934:2020, 3.1.73). The light source can include interchangeable filters for adjusting the illumination spectrum (see ISO 10934:2020, 3.1.55). In Figure A.1, the light source is shown imaged into the objective pupil in the epi-illumination Köhler geometry (see ISO 10934:2020, 3.1.73.2 and 3.1.73.3). Many instruments have adjustable light stops for controlling the size of the illumination field as well as the illumination aperture (see ISO 10934:2020, 3.1.38.6).[9]

PSI instruments use interference objectives in place of conventional microscope objectives defined in ISO 10934:2020, 3.1.106. Typically these objectives are compatible with extended, incoherent light sources.[9] Figure A.2 shows two common types of interference objective, the Michelson and Mirau type.[16][17] Other designs in common use for PSI include the Linnik objective,[18][19] and the Zygo Wide Field (ZWF) objective.[20] Table A.1 provides example specifications, including the lateral resolution according to the Sparrow criterion for a wavelength of 570 nm (see ISO 25178-600:2019, 3.3.9).

Cameras for the visible wavelengths can be of the charge-coupled device (CCD) or complementary metal-oxide semiconductor (CMOS type), with a format ranging from 300 000 pixels to over 4 million pixels. Camera selection involves not only field size and number of pixels, but also the acquisition speed, response linearity, quantum well depth, digitization resolution and the ability to shutter electronically. The net effect of the camera, optics and data processing on the topographic lateral resolution is often summarized in the instrument transfer function (ITF), defined in ISO 25178-600:2019, 3.1.19. See also References [21], [22], [23] and [24].

Adjustments upwards or downwards of the position of the objective or a sample stage (not shown in Figure A.1) bring the test surface into focus (see ISO 10934:2020, 3.1.65). Part setup usually requires a nominal adjustment of both focus and tip/tilt, although automation can complete some or all these steps (see, for example, autofocus, defined in ISO 10934:2020, 3.2.4).

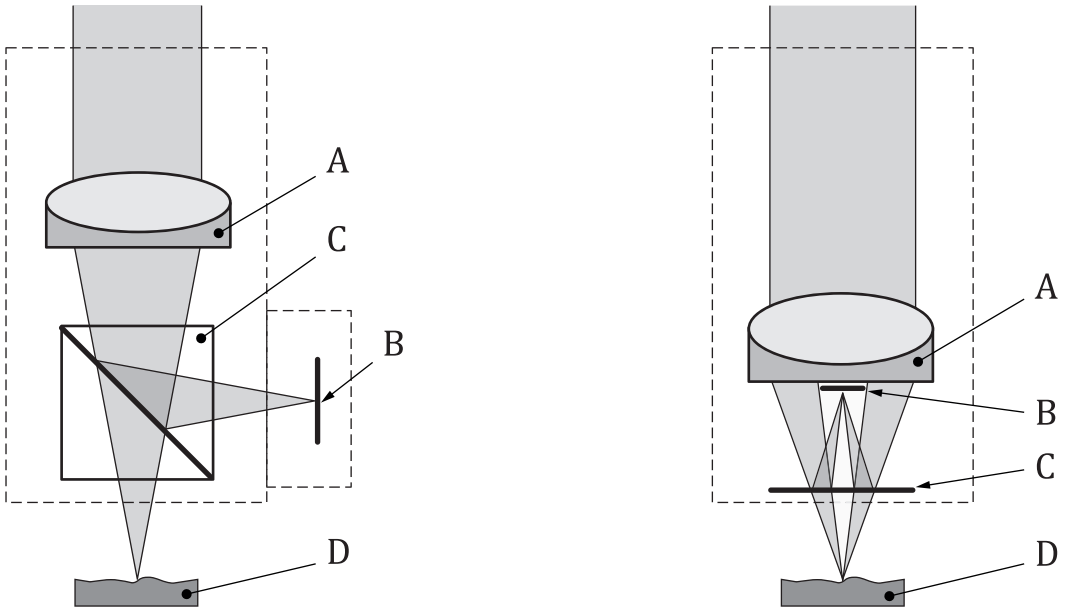

a) Michelson objective **b) Mirau objective**

Key

A lens
B reference surface
C beam splitter
D workpiece

Figure A.2 — Example types of interference microscope objectives for PSI measurements

Table A.1 — Example characteristics of interference objectives for PSI

Magnification	Type	Numerical aperture A_N	Optical lateral resolution µm
1,4×	ZWF	0,04	7,13
2,75×	Michelson	0,08	3,56
5,5×	Michelson	0,15	1,90
10×	Mirau	0,30	0,86
50×	Mirau	0,55	0,47
100×	Mirau	0,85	0,34

A.3 PSI theory of operation

Following a two-beam interference analysis,[9][25][26] the interference signal at the camera for an individual surface point of height z at a position x, y is as shown in Formula (A.1):

$$I = I_{DC} + I_{AC}\cos(\theta - \varphi + \gamma) \tag{A.1}$$

Where I_{DC} and I_{AC} are fixed coefficients, the surface-height dependent phase θ for an equivalent wavelength λ_{eq} is as shown in Formula (A.2):

$$\theta = 4\pi\frac{z}{\lambda_{eq}} \tag{A.2}$$

The phase shift imparted by a movement of the reference mirror is as shown in Formula (A.3):

$$\varphi = 4\pi\frac{\zeta}{\lambda_{eq}} \tag{A.3}$$

γ is a phase offset that is independent of z and ζ. The height is calculated from the detected phase as shown in Formula (A.4):

$$z = \frac{\lambda_{eq}}{4\pi} \tag{A.4}$$

The interference fringes correspond to lines of equal intensity and follow the surface topography as contours of equal surface height z. These fringes appear at intervals of 2π, which is equivalent in height to one-half the equivalent wavelength λ_{eq}, which for low numerical aperture systems is approximately equal to the mean value of the source emission wavelength. The phase offset γ in Formula (A.1) relates among other factors to the reflection and transmission properties of the interferometer components, as well as surface characteristics such as PCOR and thin-film effects. Inasmuch as the phase offset γ has a field dependence, it can influence the reported surface height. However, in most simple PSI measurements, the phase offset γ is assumed to be constant over the field of view and is set to zero.

In PSI, estimating the phase θ involves modulating the interference signal I through a controlled phase shift φ achieved by modulating the length ζ. In practice, these phase shifts correspond to a sequence of discrete sample intensities, as shown in Formula (A.5):

$$I_j = I_{DC} + I_{AC}\cos\left(\theta - \varphi_j\right) \tag{A.5}$$

Given that the constants I_{DC}, I_{AC} are usually unknown, at least three values are needed for φ to solve for θ. These data points represent either instantaneous acquisitions or phase steps, or more commonly, the centre points for intensity measurements integrated over the period of time between sample points, in a method commonly referred to as the "integrating bucket method".[27][28] A simple PSI algorithm uses just four samples,[10] as shown in Formula (A.6):

$$\tan(\theta) = \frac{I_2 - I_1}{I_1 - I_0} \tag{A.6}$$

where the phase shift between data acquisitions is as shown in Formula (A.7):

$$\varphi_{j+1} - \varphi_j = \frac{\pi}{2} \tag{A.7}$$

for j = 0,1,2. This is referred to as "linear PSI", in that the interference phase shift is evenly spaced in time and corresponds to a linear motion of the phase shift mechanism shown in Figure A.1.

Figure A.3 shows the interference signal and the sampling points. ISO/TR 14999-2:2019, 6.4.4, provides additional example linear PSI algorithms.

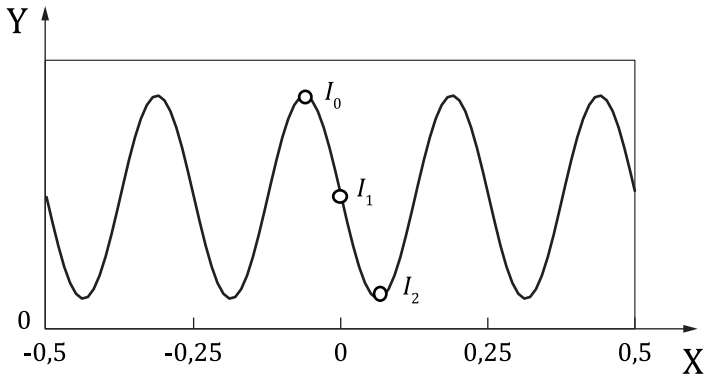

Key

X phase shift mechanism motion /µm I_0, I_1, I_2 data sample points

Y intensity

Figure A.3 — Example interference signal for linear PSI

The phase shifts φ do not need to be evenly spaced to be useful for PSI. An alternative for continuous data acquisition and averaging is sinusoidal phase shifting, a technique that has the advantage of being less demanding on phase shift mechanisms than repeated linear ramps.[29][30] The intensity pattern resulting from a sinusoidal phase shift is a superposition of multiple harmonics of the original phase modulation. Although the interference signal for a sinusoidal phase shift is very different from that of a linear phase shift, the phase shift algorithms are similar in general form, involving the arctangent of a ratio of weighted sums. An example is the four-sample algorithm[31][32] shown in Formula (A.8):

$$\tan(\theta) = \frac{I_0 + I_1 - I_2 - I_3}{I_0 - I_1 + I_2 - I_3} \tag{A.8}$$

where the phase shift is as shown in Formulae (A.9) and (A.10):

$$\varphi_j = 2{,}45 \sin\left(\eta_j + 0{,}98\right) \tag{A.9}$$

$$\eta_j = \cos\left(j\frac{\pi}{2}\right) \tag{A.10}$$

for j = 0,1,2,3.

Improvements in camera and data processing technologies together with increased performance demands have increased the number of data samples and corresponding phase shifts. Furthermore, it is now common to encounter algorithms for both linear and sinusoidal PSI with as many as 20 data acquisition samples per measurement, instead of just 3 or 4. Floating-point coefficients are now common in place of integers.[10][33][34][35] In some cases, the phase calculation involves iterative methods to compensate for errors in the phase shifting mechanism and for environmental vibrations (see Clause B.7).

The evaluation of phase θ using PSI involves the inverse of an arctangent function, which has a domain of $-\pi < \theta \leq \pi$ or a height range of $\frac{\lambda_{eq}}{2}$. It is common practice to augment this range by means of a phase unwrapping algorithm. The basic premise of phase unwrapping is that at least locally, there is continuity in the surface structure to within the 2π range, allowing for integration of the phase changes across the surface.[36] This process allows for correction of fringe-order error. ISO/TR 14999-2:2019, 6.6, provides further detailed information regarding phase unwrapping.

Annex B
(informative)

Sources of measurement error for PSI instruments

B.1 Metrological characteristics and influence quantities

ISO 25178-600:2019, 3.1.28 defines a set of metrological characteristics for areal surface topography measuring instruments. These metrological characteristics capture influence quantities, factors that can influence a measurement result and can be propagated through an appropriate measurement model to evaluate measurement uncertainty. See ISO 25178-700 and ISO 12179 for methods for calibration, adjustment and verification of the metrological characteristics.

In this annex, influence quantities are described that affect the metrological characteristics. Knowledge of these influence quantities is not needed for uncertainty analysis if it is feasible to perform a direct calibration of the corresponding metrological characteristics. However, knowledge of influence quantities can be useful for optimizing measurements and minimizing sources of error.

Table B.1 summarizes the influence quantities discussed in this annex.

Table B.1 — Summary of influence quantities and related metrological characteristics

Item	Influence quantity	Relevant metrological characteristic
B.2	Equivalent wavelength	α_z amplification coefficient
B.3	Cyclic errors in the phase calculation	l_z linearity deviation T_{FI} topography fidelity
B.4	Focus effects	l_z linearity deviation W_{R} topographic spatial resolution
B.5	Reference mirror flatness	z_{FLT} flatness deviation
B.6	Optical ray tracing error	z_{FLT} flatness deviation $\Delta x(x,y), \Delta y(x,y)$ *x-y* mapping deviation
B.7	Random environmental vibration	N_{M} measurement noise
B.8	Camera noise	N_{M} measurement noise
B.9	Optical lateral resolution	W_{R} topographic spatial resolution
B.10	Sampling interval	W_{R} topographic spatial resolution
B.11	Optical distortion	$\Delta x(x,y), \Delta y(x,y)$ *x-y* mapping deviation
B.12	Surface films	T_{FI} topography fidelity
B.13	Dissimilar materials	T_{FI} topography fidelity
B.14	Surface slopes and discrete step features	T_{FI} topography fidelity

B.2 Equivalent wavelength

The PSI method relies on the equivalent wavelength λ_{eq} as the fundamental scaling factor for the conversion of phase to surface height, as given in Formula (A.4). The equivalent wavelength can be calculated from contributions such as the light source wavelength together with other factors related to the instrument design, including the effects of camera spectral sensitivity and the illumination geometry at high numerical apertures.[37][38] Alternatively, the wavelength λ_{eq} can be calibrated implicitly as part of a calibration procedure for the amplification coefficient α_z using a material measure.[39][40] The ratio of the equivalent wavelength to the mean light source wavelength is often referred to as the “obliquity factor”. In laser Fizeau or comparable systems with well-known source wavelengths and low numerical apertures, it is often sufficient to equate the equivalent wavelength to the source wavelength.[41]

The equivalent wavelength is an influence quantity for the amplification coefficient α_z defined in ISO 25178-600:2019, 3.1.10.

B.3 Cyclic errors in the phase calculation

Several error mechanisms produce linearity deviations that are harmonics of the interference signal and can be associated with the PSI algorithm. These include motion errors in the phase shifting mechanism, camera nonlinearity and synchronous vibrations, and can manifest themselves as false topographical features, sometimes known as "ripple", that follow the interference fringe pattern. These errors have been studied[42][43][44] and can also be quantified experimentally, by adjusting the sample tilt to change the fringe pattern or fringe density, or both.

Cyclic errors are influence quantities for the linearity deviation l_z defined in ISO 25178-600:2019, 3.1.11, as well as for the topography fidelity T_{FI} defined in ISO 25178-600:2019, 3.1.26.

B.4 Focus effects

The PSI measurement principle assumes that the entire sample surface is at the position of best imaging focus, and that this position is also characterized by the maximum interference fringe contrast. If the sample is inadequately positioned for best focus, or if the surface topography exceeds the depth of field of the imaging system, there can be distortions in the height response that produce linearity deviations.[45][46][47]

Focus effects are influence quantities for the linearity deviation l_z defined in ISO 25178-600:2019, 3.1.11, as well as for the topographic spatial resolution W_{R} defined in ISO 25178-600:2019, 3.1.20.

B.5 Reference mirror flatness

For PSI instruments as described in Annex A, the interference pattern is a measure of the difference between the sample surface topography and a reference flat, also referred to as an "area reference", as defined in ISO 25178-600:2019, 3.1.1. Therefore, the topography of the reference flat is relevant to accurately measuring surface topography with respect to the area reference.[48][49]

Reference mirror flatness is an influence quantity for the flatness deviation z_{FLT} defined in ISO 25178-600:2019, 3.1.12.

B.6 Optical ray tracing error

In practice, imperfections in the optical system can have a similar effect to form deviations of the reference flat. These contributions are difficult to distinguish and are often calibrated at the same time. However, flatness deviations arising from optical imperfections can depend on both local slope and the overall orientation of the sample part.

Optical ray tracing error is an influence quantity for the flatness deviation z_{FLT} defined in ISO 25178-600:2019, 3.1.12, as well as for $x - y$ mapping deviation $\Delta x(x,y)$, $\Delta y(x,y)$ defined in ISO 25178-600:2019, 3.1.13.

B.7 Random environmental vibration

A PSI instrument performs best in an environment isolated from sources of vibration. Often, the instrument is placed on a vibration isolation table, e.g. a rigid slab supported on air-damped legs. The effect of vibration depends strongly on its frequency. Vibrational frequencies well below the camera framerate generate distortions in form and waviness as a function of sample part orientation, whereas higher frequencies generate cyclic errors that vary from measurement to measurement.[50] The effect of vibrations on specific PSI algorithms and data acquisition methods has been studied in detail for both linear and sinusoidal PSI.[31][43] Some PSI methods can interpret the interference signals to calculate phase even in the presence of vibrations and air turbulence.[51][52]

Environmental vibration is an influence quantity for the measurement noise N_M defined in ISO 25178-600:2019, 3.1.15.

B.8 Camera noise

In PSI, the imaging camera is a dominant source of random instrument noise N_I (see ISO 25178-600:2019, 3.1.14). The effect of camera noise on the measurement is a function of the data acquisition time, or equivalently, the number of data samples in the PSI algorithm, as well as the number of averages for the measurement.[31][53][54]

Camera noise is an influence quantity for the measurement noise N_M defined in ISO 25178-600:2019, 3.1.15.

B.9 Optical lateral resolution

The lateral resolution depends, among other factors, on the configuration of the lenses, mirrors, light source bandwidth and degree of coherence of the optical system. ISO 25178-600:2019, 3.3, defines optical lateral resolution parameters based on traditional imaging, including the Raleigh criterion, the Sparrow criterion and the Abbe resolution limit, which relate uniquely to the ability of an optical system to clearly separate closely-spaced image features.

Lateral resolution of the optical system is an influence quantity for the topographic spatial resolution W_R defined in ISO 25178-600:2019, 3.1.20.

B.10 Sampling interval

As defined in this document, an electronic camera is a 2D detector array comprised of imaging pixels that map to the sample surface, forming an x, y grid of image points. In object space, i.e. the coordinates of the surface points, the spacing between neighbouring image points is referred to in ISO 25178-600:2019, 3.1.17, as the "sampling interval D_x, D_y", also known as the "lateral sampling interval", "spatial sampling", "lateral sampling" or variants of these terms. An additional factor related to the camera array is the size of the pixels, which map to areas of integration on the sample surface.

The size of the sampling interval depends on the optical magnification and on the physical dimensions of the camera detector array. The sampling interval is a common instrument specification that varies with the selected interference objective. If the sampling interval is comparable to or larger than the optical lateral resolution, then the lateral sampling can be a significant influence quantity in determining the topographic spatial resolution.

Electronic firmware or data processing software can alter the sampling interval if these system components result in correlation between reported values for neighbouring camera pixels. This can be the case with default noise filtering, or because of a measurement process that includes information from multiple pixels to determine the height of a single image point.

The lateral sampling of the optical system is an influence quantity for the topographic spatial resolution W_R defined in ISO 25178-600:2019, 3.1.20.

B.11 Optical distortion

Distortion is an imaging characteristic for an optical system, related both to the approximations inherent in ray tracing through systems far from the optical axis and imperfections in the optical design.[55][56] Common types of distortion include barrel distortion (see ISO 10934:2020, 3.1.4.5.1) and pincushion distortion (see ISO 10934:2020, 3.1.4.5.2).

Optical distortion is an influence quantity for the x-y mapping deviation $\Delta x(x,y)$, $\Delta y(x,y)$ defined in ISO 25178-600:2019, 3.1.13.

B.12 Surface films

A surface film is defined in ISO 25178-600:2019, 3.4.1, as a material deposited onto another surface whose optical properties are different from that surface. Films are common in many applications, either by direct deposition as part of manufacturing, as a temporary consequence of the manufacturing process (e.g. an oil film), or through a natural process such as oxidation.

Surface films can significantly affect the response of PSI instruments. Surface films have a first-order effect on the phase offset γ in Formula (A.1), meaning that the measured phase from the PSI measurement can depend to the same degree on the optical properties of the film as on the surface height. Surface film effects have been studied to determine their influence on PSI and to develop methods for interpreting their influence on areal surface topography measurements.[57][58][59]

The effect of surface films is an influence quantity for the topography fidelity T_{FI} defined in ISO 25178-600:2019, 3.1.26.

B.13 Dissimilar materials

As with surface films, the optical properties of the sample materials can have a significant impact on the reported phase as a function of surface position. The PCOR for dissimilar materials has a first-order effect on the phase offset γ in Formula (A.1), meaning that the measured phase from the PSI measurement can depend to the same degree on the PCOR as on the surface height.[11][60] This can result in part-dependent uncertainty contributions, particularly for optically non-uniform materials (see ISO 25178-600:2019, 3.4.6).

The effect of dissimilar materials is an influence quantity for the topography fidelity T_{FI} defined in ISO 25178-600:2019, 3.1.26.

B.14 Surface slopes and discrete step features

The simple Formula (A.4) for converting interference phase as measured by PSI to surface height is based on a highly simplified model of the instrument that has limitations.[61] In particular, the effect of surface slopes that deflect the incident light at an angle through the optical system produces measurement errors that are not quantified using routine calibrations available for other metrological characteristics.[62] Theoretical models[63][64][65][66] and experimental methods have been developed,[67][68] but calibration procedures have not been standardized.

The effect of surface slopes and discrete step features is an influence quantity for the topography fidelity T_{FI} defined in ISO 25178-600:2019, 3.1.26.

Annex C
(informative)

Relationship to the GPS matrix model

C.1 General

The ISO GPS matrix model given in ISO 14638 gives an overview of the ISO GPS system of which this document is a part.

The fundamental rules of ISO GPS given in ISO 8015 apply to this document and the default decision rules given in ISO 14253-1 apply to specifications made in accordance with this document unless otherwise indicated.

C.2 Information about this document and its use

This document specifies the methods, specific terminology and exemplary influence quantities for phase shifting interferometry instruments used to measure profile and areal surface texture.

C.3 Position in the GPS matrix model

This document is a general ISO GPS standard which influences chain link F of the chains of standards on profile and areal surface texture in the GPS matrix model as shown in Table C.1. The rules and principles given in this document apply to all segments of the ISO GPS matrix which are indicated with a filled dot (•).

Table C.1 — Relationship to the ISO GPS matrix model

	Chain links						
	A	B	C	D	E	F	G
	Symbols and indications	Feature requirements	Feature properties	Conformance and non-conformance	Measurement	Measurement equipment	Calibration
Size							
Distance							
Form							
Orientation							
Location							
Run-out							
Profile surface texture						•	
Areal surface texture						•	
Surface imperfections							

C.4 Related International Standards

The related International Standards are those of the chains of standards indicated in Table C.1.

Bibliography

[1] ISO 8015, *Geometrical product specifications (GPS) — Fundamentals — Concepts, principles and rules*

[2] ISO 10934:2020, *Microscopes — Vocabulary for light microscopy*

[3] ISO 14253-1, *Geometrical product specifications (GPS) — Inspection by measurement of workpieces and measuring equipment — Part 1: Decision rules for verifying conformity or nonconformity with specifications*

[4] ISO 14638, *Geometrical product specifications (GPS) — Matrix model*

[5] ISO/TR 14999-1, *Optics and photonics — Interferometric measurement of optical elements and optical systems — Part 1: Terms, definitions and fundamental relationships*

[6] ISO/TR 14999-2:2019, *Optics and photonics — Interferometric measurement of optical elements and optical systems — Part 2: Measurement and evaluation techniques*

[7] ISO 25178-607:2019, *Geometrical product specifications (GPS) — Surface texture: Areal — Part 607: Nominal characteristics of non-contact (confocal microscopy) instruments*

[8] ISO 25178-700, *Geometrical product specifications (GPS) — Surface texture: Areal — Part 700: Calibration, adjustment and verification of areal topography measuring instruments*

[9] P. de Groot, "Principles of interference microscopy for the measurement of surface topography," Advances in Optics and Photonics **7**, 1-65 (2015).

[10] H. Schreiber, and J. H. Bruning, "Phase Shifting Interferometry," in *Optical Shop Testing,* edited by D. Malacara, pp. 547-666, (John Wiley & Sons, Inc., 2006).

[11] P. de Groot, "Phase Shifting Interferometry," in *Optical Measurement of Surface Topography,* edited by R. Leach, chapt.8, pp. 167-186, (Springer Verlag, Berlin, 2011).

[12] K. Creath, and J. Schmit, "Phase-Measurement Interferometry," in *Encyclopedia of Modern Optics,* edited by R. D. Guenther, pp. 364-374, (Elsevier, Oxford, 2005).

[13] K. Creath, "Phase-Measurement Interferometry Techniques," in *Progress in Optics,* edited by E. Wolf, Vol.26, chapt. 5, pp. 349-393, (Elsevier Science Publishers, Amsterdam, 1988).

[14] M. V. Mantravadi, and D. Malacara, "Newton, Fizeau, and Haidinger Interferometers," in *Optical Shop Testing,* edited by D. Malacara, pp. 1-45, (Wiley-Interscience, Hoboken, 2007).

[15] P. de Groot, "Fizeau interferometer," in *Light: Introduction to Optics and Photonics,* edited by J. F. Donnelly and N. M. Massa, chapt. 8.7.2, pp. 180-184, (New England Board of Higher Education, 2010).

[16] W. Krug, J. Rienitz, and G. Schulz, *Contributions to Interference Microscopy*, (Hilger & Watts, London, 1964).

[17] A.H. Mirau "Interferometer," US Patent 2,612,074 (1949).

[18] V. P. Linnik, "Ein apparat fur mikroskopisch-interferometrische untersuchung reflektierender objekte (mikrointerferometer)," Doklady Akademiya Nauk S.S.S.R., 18–23 (1933).

[19] K. Creath, *Dynamic phase imaging utilizing a 4-dimensional microscope system*, (SPIE, 2011) PWB.

[20] P. J. de Groot, and J. F. Biegen, "Interference microscope objectives for wide-field areal surface topography measurements," Optical Engineering **55**, 074110-074110 (2016).

[21] P. de Groot, X. Colonna de Lega "Interpreting interferometric height measurements using the instrument transfer function", Proc. FRINGE 30-37 (2006).

[22] E. Church, and P. Takacs, “Effects Of The Optical Transfer Function In Surface Profile Measurements”, Proc. SPIE **1164**, 2-15 (1989).

[23] P. J. de Groot, “The instrument transfer function for optical measurements of surface topography,” Journal of Physics: Photonics **3**, 024004 (2021).

[24] R. Su, J. M. Coupland, C. J. R. Sheppard, and R. K. Leach, “Scattering and three-dimensional imaging in surface-topography measuring interference microscopy,” Journal of the Optical Society of America A **38**, 27-42 (2020).

[25] P. Hariharan, *Optical interferometry*, (Academic Press, 2003).

[26] D. A. Page, “Interferometry,” in *Handbook of Optical Metrology,* edited by T. Yoshizawa, chapt. 6, pp. 191-218, (CRC Press, Boca Raton, FL, 2009).

[27] J. C. Wyant, “Use of an ac heterodyne lateral shear interferometer with real-time wavefront correction systems,” Applied Optics **14**, 2622-2626 (1975).

[28] J. E. Greivenkamp, “Generalized Data Reduction For Heterodyne Interferometry,” Optical Engineering **23**, 234350 (1984).

[29] O. Sasaki, H. Okazaki, and M. Sakai, “Sinusoidal phase modulating interferometer using the integrating-bucket method,” Appl Opt **26**, 1089-93 (1987).

[30] A. Dubois, “Phase-map measurements by interferometry with sinusoidal phase modulation and four integrating buckets,” Journal of the Optical Society of America A **18**, 1972 (2001).

[31] P. de Groot, “Design of error-compensating algorithms for sinusoidal phase shifting interferometry,” Applied Optics **48**, 6788 (2009).

[32] P. de Groot “Error compensation in phase shifting interferometry,” US Patent 7,948,637 (2011).

[33] K. Freischlad, and C. L. Koliopoulos, “Fourier description of digital phase-measuring interferometry,” Journal of the Optical Society of America A **7**, 542-551 (1990).

[34] Y. Surrel, “Design of algorithms for phase measurements by the use of phase stepping,” Appl Opt **35**, 51-60 (1996).

[35] M. Strojnik, R. Hanayama, K. Hibino, and G. Paez, “Error estimation of phase detection algorithms and comparison of window functions,” in *Interferometry XVI: Techniques and Analysis*, Proc. SPIE **8511** pp.84930J-84930J-8 (2012).

[36] D. C. Ghiglia, and M. D. Pritt, *Two-Dimensional Phase Unwrapping, Theory, Algorithms, and Software*, (John Wiley & Sons, New York, 1998).

[37] G. Schulz, and K.-E. Elssner, “Errors in phase-measurement interferometry with high numerical apertures,” Applied Optics **30**, 4500 (1991).

[38] J. F. Biegen, “Calibration requirements for Mirau and Linnik microscope interferometers,” Applied Optics **28**, 1972 (1989).

[39] P. de Groot, and D. Fitzgerald, “Measurement, certification and use of step-height calibration specimens in optical metrology”, Proc. SPIE **10329**, 1032919.1-1032919.9 (2017).

[40] M. Greve, R. Krüger-Sehm “Direct determination of the aperture correction factor of interference microscopes,” in *Proceedings of the XI. International Colloquium on Surfaces*, Proceedings of the XI. International Colloquium on Surfaces **Part 1** pp.156-163 (2004).

[41] J. F. Biegen, and R. A. Smythe, “High Resolution Phase Measuring Laser Interferometric Microscope For Engineering Surface Metrology,” in *Surface Measurement and Characterization*, Proc. SPIE **1009** pp.35-45 (1989).

[42] J. Schwider, R. Burow, K. E. Elssner, J. Grzanna, R. Spolaczyk, and K. Merkel, "Digital wave-front measuring interferometry: some systematic error sources," Applied Optics **22**, 3421 (1983).

[43] P. J. de Groot, "Vibration in phase-shifting interferometry," Journal of the Optical Society of America A **12**, 354-365 (1995).

[44] K. Creath, *Comparison Of Phase-Measurement Algorithms*, (SPIE, 1987) OP.

[45] S. Chakmakjian, J.F. Biegen, P. de Groot "Simultaneous focus and coherence scanning in interference microscopy", IWI Proceedings 171-172 (1996).

[46] A. Dubois, J. Selb, L. Vabre, and A.-C. Boccara, "Phase Measurements With Wide-Aperture Interferometers," Applied Optics **39**, 2326 (2000).

[47] R. Su, M. Thomas, R. K. Leach, and J. Coupland, "Effects of defocus on the transfer function of coherence scanning interferometry," Optics Letters **43**, 82-85 (2018).

[48] K. Creath, and J. C. Wyant, "Absolute measurement of surface roughness," Applied Optics **29**, 3823 (1990).

[49] C. L. Giusca, R. K. Leach, F. Helary, T. Gutauskas, and L. Nimishakavi, "Calibration of the scales of areal surface topography-measuring instruments: part 1. Measurement noise and residual flatness," Measurement Science and Technology **23**, 035008 (2012).

[50] P. J. de Groot, "Interference Microscopy for Surface Structure Analysis," in *Handbook of Optical Metrology,* edited by T. Yoshizawa, chapt. 31, pp. 791-828, (CRC Press, 2015).

[51] L. L. Deck, "Model-based phase shifting interferometry," Applied Optics **53**, 4628-4636 (2014).

[52] F. Munteanu, and J. Schmit, "Iterative least square phase-measuring method that tolerates extended finite bandwidth illumination," Applied Optics **48**, 1158-1167 (2009).

[53] C. P. Brophy, "Effect of intensity error correlation on the computed phase of phase-shifting interferometry," Journal of the Optical Society of America A **7**, 537 (1990).

[54] P. de Groot, and J. DiSciacca, "Surface-height measurement noise in interference microscopy", Proc. SPIE **10749**, 107490Q-1 - 107490Q-9 (2018).

[55] W. J. Smith, *Modern Optical Engineering*, (SPIE Press, Bellingham, WA, 2007).

[56] P. Ekberg, R. Su, and R. Leach, "High-precision lateral distortion measurement and correction in coherence scanning interferometry using an arbitrary surface," Optics Express **25**, 18703-18712 (2017).

[57] M. F. Fay, and T. Dresel, "Applications of model-based transparent surface films analysis using coherence-scanning interferometry," Optical Engineering **56**, 111709.1-6 (2017).

[58] J. Park, J.-A. Kim, H. Ahn, J. Bae, and J. Jin, "A Review of Thickness Measurements of Thick Transparent Layers Using Optical Interferometry," International Journal of Precision Engineering and Manufacturing, (2019).

[59] P. J. de Groot, and X. Colonna de Lega, "Signal modeling for modern interference microscopes", Proc. SPIE **5457**, 26-34 (2004).

[60] J. M. Bennett, "Precise Method for Measuring the Absolute Phase Change on Reflection," Journal of the Optical Society of America **54**, 612 (1964).

[61] P. de Groot, X. Colonna de Lega, R. Su, and R. K. Leach, "Does interferometry work? A critical look at the foundations of interferometric surface topography measurement", Proc. SPIE **11102**, 111020G.1 - 111020G-11 (2019).

[62] R.K. Leach, P.J. de Groot, H. Haitjema "Infidelity and the calibration of surface topography measuring instruments", Proc. ASPE 1-7 (2018).

[63] J. Coupland, and N. Nikolaev, "Surface scattering and the 3D transfer characteristics of optical profilers", (SPIE, 2020).

[64] P. de Groot, and X. Colonna de Lega, “Fourier optics modelling of interference microscopes,” J. Opt. Soc. Am. A **37**, B1-B10 (2020).

[65] R. K. Leach, C. Giusca, H. Haitjema, C. Evans, and X. Jiang, “Calibration and verification of areal surface texture measuring instruments”, CIRP Annals - Manufacturing Technology **64**, 797-813 (2015).

[66] Y. Zhou, J. Troutman, C. J. Evans, and A. D. Davies, “Using the random ball test to calibrate slope dependent errors in optical profilometry”, OSA Technical Digest (online) OW4B.2 (2014).

[67] L. L. Deck, and C. Evans, “High performance Fizeau and scanning white-light interferometers for mid-spatial frequency optical testing of free-form optics”, Proc. SPIE **5921**, 59210A-59210A-8 (2005).

[68] X. Colonna de Lega, T. Dresel, J. Liesener, M. Fay, N. Gilfoy, K. Delldonna et al. “Optical form and relational metrology of aspheric micro optics”, Proc. ASPE **67**, 20-23 (2017).

[69] ISO 12179, *Geometrical product specifications (GPS) — Surface texture: Profile method — Calibration of contact (stylus) instruments*

ICS 17.040.20
Price based on 18 pages